


Homology Modelling and Molecular Docking Studies of Selected Substituted Benzo[d]imidazol-1-yl)methyl) benzimidamide Scaffolds on *Plasmodium falciparum* Adenylosuccinate Lyase Receptor

Bioinformatics and Biology Insights
Volume 13: 1–10
© The Author(s) 2019
Article reuse guidelines:
sagepub.com/journals-permissions
DOI: 10.1177/1177932219865533



Gbolahan O Oduselu^{1,2}, Olayinka O Ajani^{1,2} , Yvonne U Ajamma¹, Benedikt Brors³ and Ezekiel Adebiyi^{1,3,4} 

¹Covenant University Bioinformatics Research (CUBRe), Covenant University, Ota, Nigeria.

²Department of Chemistry, College of Science and Technology, Covenant University, Ota,

Nigeria. ³Division of Applied Bioinformatics, German Cancer Research Center (DKFZ),

Heidelberg, Germany. ⁴Department of Computer and Information Science, Covenant University,

Ota, Nigeria.

ABSTRACT: *Plasmodium falciparum* adenylosuccinate lyase (*PfADSL*) is an important enzyme in purine metabolism. Although several benzimidazole derivatives have been commercially developed into drugs, the template design as inhibitor against *PfADSL* has not been fully explored. This study aims to model the 3-dimensional (3D) structure of *PfADSL*, design and predict in silico absorption, distribution, metabolism, excretion and toxicity (ADMET) of 8 substituted benzo[d]imidazol-1-yl)methyl)benzimidamide compounds as well as predict the potential interaction modes and binding affinities of the designed ligands with the modelled *PfADSL*. *PfADSL* 3D structure was modelled using SWISS-MODEL, whereas the compounds were designed using ChemDraw Professional. ADMET predictions were done using OSIRIS Property Explorer and Swiss ADME, whereas molecular docking was done with AutoDock Tools. All designed compounds exhibited good in silico ADMET properties, hence can be considered safe for drug development. Binding energies ranged from -6.85 to -8.75 kcal/mol. Thus, they could be further synthesised and developed into active commercial antimalarial drugs.

KEYWORDS: ADMET prediction, malaria, benzimidazole, antimalarial activity, molecular docking, drug target, benzimidamide, in silico

RECEIVED: June 24, 2019. **ACCEPTED:** June 29, 2019.

TYPE: Computational Modeling Protein Structures & Interactions- Original Research

FUNDING: The author(s) disclosed receipt of the following financial support for the research, authorship, and/or publication of this article: This work was supported by the Fogarty National Institutes of Health Common Fund (Grant No: 1U2RTW010679) and Alexander von Humboldt (AvH) Senior Georg Forster for EA.

DECLARATION OF CONFLICTING INTERESTS: The author(s) declared no potential conflicts of interest with respect to the research, authorship, and/or publication of this article.

CORRESPONDING AUTHOR: Ezekiel Adebiyi, Covenant University Bioinformatics Research (CUBRe), Covenant University, Km 10 Idiroko Road, P.M.B. 1023, Ota, Ogun State, Nigeria. Email: ezekiel.adebiyi@covenantuniversity.edu.ng

Introduction

Malaria is one of the most challenging infectious diseases to eradicate, especially in Sub-Saharan Africa.¹ *Plasmodium falciparum* remains the most prevalent malaria parasite in the world accounting for 216 million estimated cases in 2016.² The drug resistance of malaria parasite has led to the need and search for new chemical scaffolds that have novel modes of action and can act through new protein targets.^{3,4} One of such protein targets in *Pfalciparum* is the adenylosuccinate lyase (ADSL), which is an important enzyme in purine metabolism.⁵ The de novo purine biosynthetic pathway that gives rise to the formation of adenosine monophosphate (AMP), catalysed by ADSL, is absent in *Pfalciparum*, making it a potential drug target for antimalarial studies.^{6,7} Cassera et al⁷ reported that 5-aminoimidazole-4-carboxamide ribonucleotide (AICAR) and its analogues can serve as potential inhibitors for ADSL of *Pfalciparum*, hence novel putative antiparasitic agents. Benzimidazole derivatives (substituted benzo[d]imidazol-1-yl)methyl)benzimidamides) were considered as potential analogues for AICAR due to similarities in chemical structure (Figure 1), and could be evaluated for their antimalarial propensity. Benzimidazole derivatives have been widely used in recent years due to their wide range of pharmacological activities including antimalarial,⁸ antileishmanial,⁹ analgesics,¹⁰ anticancer,¹¹ antitumour,¹² antimicrobial,¹³ anti-inflammatory,¹⁴ antihepatitis C

virus,¹⁵ antihelminthic,¹⁶ antibacterial¹⁷ and antitrypanosomal¹⁸ activities. Although several benzimidazole derivatives have been synthesised and developed into commercially available drugs, little is known about the design of the template as an inhibitor against *Pfalciparum* ADSL (*PfADSL*).

Over the years, different approaches have been used to improve how antimalarial agents are designed, put through clinical trials and eventually released as commercially available drugs.¹⁹ One of such approaches is structure-based drug design (SBDD), which relies on the knowledge of the 3-dimensional (3D) structure of the protein target to design a suitable ligand that can function as its potential inhibitor.²⁰ In a situation where the experimental 3D structure of the protein is not available, homology model can be built from its amino acid sequence.²¹ Molecular docking is an important technique in SBDD, which can be applied in facilitating and speeding up the development of antimalarial agents or drugs that can be active against the deadly malaria parasite.²² Molecular docking has helped scientists to virtually screen a library of ligands (or compounds) against a target protein and predict the binding conformations and affinities of the ligands to the target.¹⁹ The aim of this study is to model the 3D structure of *PfADSL*, design and predict the in silico absorption, distribution, metabolism, excretion and toxicity (ADMET) of some substituted



benzo[*d*]imidazol-1-yl)methyl)benzimidamide compounds as well as predict the potential interaction modes and binding affinities of the designed ligands with the modelled *PfADSL*.

Materials and Methods

Homology modelling of PfADSL and the target-template sequence alignment

The experimental crystal structure of *PfADSL* is not available in the Protein Data Bank (PDB);²³ hence, its 3D structure was modelled. The protein ID of the target (*P. falciparum* adenylosuccinate lyase 3D7 strain) was retrieved from UniProt Knowledgebase (UniProtKB)²⁴ with the accession number Q7KWJ4. Afterwards, the protein ID was submitted to SWISS-MODEL²⁵ web server to develop a model with sufficient query sequence coverage and sequence identity. The most reliable 3D structure was selected based on the Global Model Quality Estimation (GMQE)²⁶ and Qualitative Model Energy Analysis (QMEAN)²⁷ values. The GMQE values are usually between 0 and 1, and the higher the number, the higher the reliability of the predicted structure, while for QMEAN, a value below 4.0 shows reliability.²⁸ The similarity identity between the amino acid sequences of the homology model of *PfADSL* and the template structure used for the homology model were confirmed using Clustal Omega version 1.2.1.²⁹

Structure validation of modelled protein

The SWISS-MODEL web server automatically calculates the QMEAN scoring function for the estimation of the local and the global model quality based on the geometry, the interactions and the solvent potential of the protein model. It also provides the z-score ranging from 0 to 1, which are compared with the expected value for any structure. PROCHECK was used to check for the quality of the modelled 3D structure of *PfADSL* generated via SWISS-MODEL. For this structure validation, the .pdb file format of the modelled *PfADSL* was uploaded on the PDBsum web server³⁰ of European Bioinformatics Institute. The .pdb file format of the modelled *PfADSL* was uploaded on the server to obtain both the Ramachandran plot and the Ramachandran plot statistics. While the Ramachandran plot is used in accessing the quality of a modelled protein or an experimental structure, the Ramachandran plot statistics provides information on the total number of amino acid residues found in the favourable, allowed and disallowed regions.³¹ Also, Verify3D³² was used to validate the structure of the modelled protein, determine how compatible a 3D structure is to its own amino acids and compare the result with that of good-known structures.

Alignment of the PfADSL model and the template structure

The alignment of the *PfADSL* model and template structure was carried out using PyMOL molecular viewer³³ to show how

closely related the carbon atoms are. This is derived from the root mean square deviation (RMSD) between the positioning of the carbon atoms of both the template and the model that is obtained from the alignment. The lower the RMSD (w.r.t 0), the more closely related the structures are.

Ligand modelling

AICAR analogues are good inhibitors of *PfADSL*⁷ and similar to benzimidazole, as shown in Figure 1. Therefore, the benzimidazole derivatives were built as ligands to function as potential inhibitors of *PfADSL*, which is the target protein. The 2-dimensional (2D) structures of the substituted benzo[*d*]imidazol-1-yl)methyl)benzimidamide compounds, **4a-h** (Scheme 1), were built using ChemDraw Professional 15.0 by PerkinElmer USA. Also, ChemDraw was used to generate the simplified molecular-input line-entry system (SMILES) that were converted to their corresponding 3D structures using FRee Online druG 3D conformation generator (FROG)³⁴ and saved in .pdb format. In addition, OpenBabel software³⁵ was used to convert the .pdb files to the AutoDock docking format (.pdbqt), which was further used for the docking simulation.

In silico drug-likeness and toxicity predictions

Drug-likeness is a prediction that determines whether a particular pharmacological agent has properties consistent with being an orally active drug.³⁶ This prediction is based on an already established concept by Lipinski et al,³⁷ called Lipinski rule of five. The rule predicts that there is likely to be poor absorption or permeation when a compound possesses more than 5H-bond donors, 10H-bond acceptors, molecular weight greater than 500 and the calculated LogP (CLogP) greater than 5.³⁷ The selection of compounds as drug candidates is also determined by a parameter called drug score.³⁸ The higher the drug score value, the higher the chance of the compound being considered as a drug candidate.³⁸ The *in silico* drug-likeness and toxicity predictions of the designed ligands were carried out using OSIRIS Property Explorer³⁹ and Swiss ADME predictor.^{40,41} OSIRIS Property Explorer programme estimates the mutagenic, tumorigenic, irritant and reproductive risks, and also provides information on the compound's hydrophilicity (LogP), solubility (LogS), molecular weight, drug-likeness and drug score.⁴² Meanwhile, SwissADME predictor provides information on the numbers of hydrogen donors, hydrogen acceptors and rotatable bonds, total polar surface area and the synthetic accessibility of the compounds. The ligands were also subjected to Lipinski et al,³⁷ Muegge et al,⁴³ Ghose et al,⁴⁴ Egan et al⁴⁵ and Veber et al⁴⁶ screenings using SwissADME predictor. The analyses of the compounds were compared with that of chloroquine, and only compounds without violation of any of the screenings were used for the molecular docking analysis.

Protein preparation

The homology modelled 3D structure of the target protein, PfADSL, was downloaded from SWISS-MODEL in its .pdb format. The modelled protein structure was defined as receptor while the complexed ligands were removed using Chimera software.⁴⁷ Furthermore, the protein was prepared by the computation of Gasteiger charges, with the addition of polar hydrogens and merging of the nonpolar hydrogens using AutoDockTools 1.5.6.⁴⁸

Prediction of active sites in the modelled protein

The Computed Atlas of Surface Topography of proteins (CASTp) 3.0⁴⁹ was used to predict the active sites that were present in the modelled protein structure. CASTp is an online

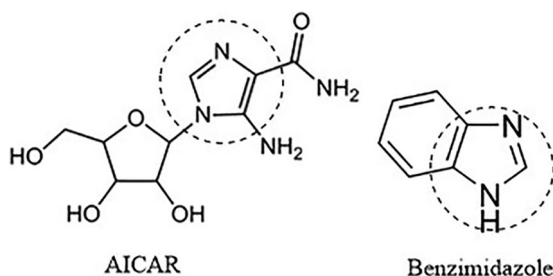


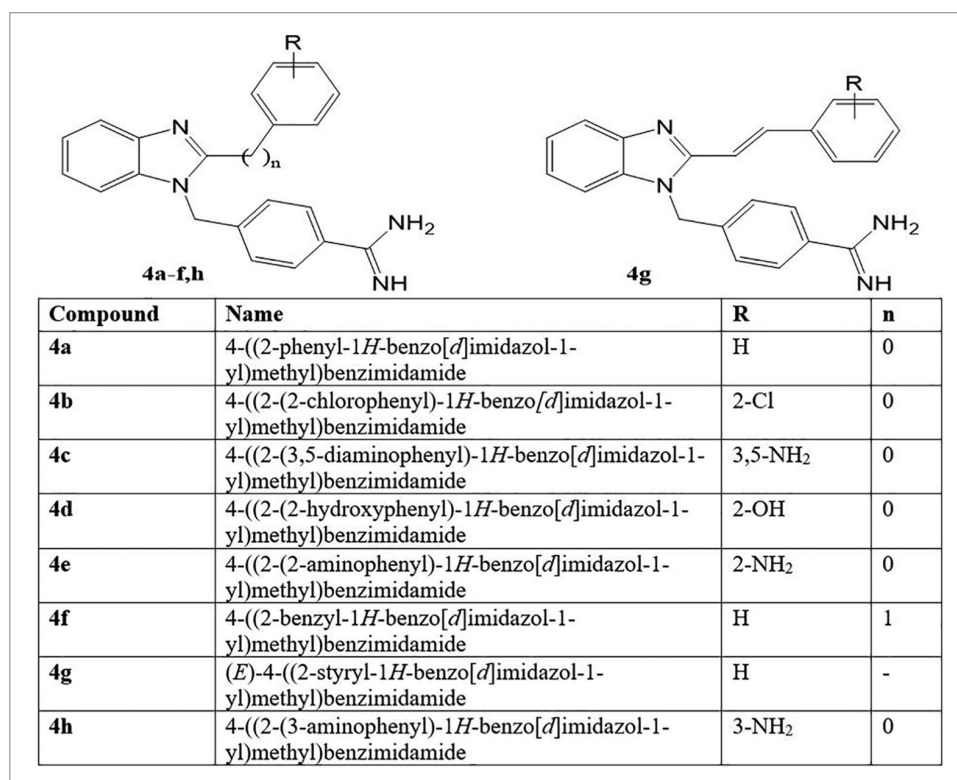
Figure 1. Structures of AICAR and benzimidazole showing the regions of similarity.

Abbreviation: AICAR, 5-aminoimidazole-4-carboxamide ribonucleotide.

server that is applied in the identification and measurement of voids on 3D protein structures.⁵⁰ The modelled 3D protein was submitted on the server, and the necessary amino acids for binding interactions were predicted.⁵⁰

Molecular docking analysis

It has been reported that ADSL enzymes, which were used for the docking analyses, are biologically active as homotetramers.^{51,52} The molecular docking studies were carried out using AutoDockTools, which is a free graphic user interface (GUI) for the AutoDock4.2 programme.⁵³ The grid box was constructed using 58, 58, and 40, pointing in x, y, and z directions, respectively, with a grid point spacing of 0.508 Å. The centre grid box is of 14.527 Å, 56.689 Å and -5.122 Å around Arg 17A, Tyr 18A, Asn 312A, His 173C, Asn 90D, Asp 92D, Gln 250D, Arg 338D, Ser 343D and Arg 347D. These amino acids were selected based on the CASTp result and the alignment of the modelled 3D structure to the template structure. In addition, the docking analysis was executed using Lamarckian Genetic Algorithm 4.2, and the macromolecule was kept rigid throughout the docking simulation. The number of genetic algorithm runs was set at 10, and the other docking parameters were left at default values. Ten different conformations were generated for each ligand scored using AutoDock 4.2 scoring functions and were ranked according to their binding energies. AutoDockTools, PyMOL and LigPlot⁵⁴ were used for the post-docking analyses.



Scheme 1. Schematic representation of the compounds 4a-h.

'R' stands for substituents on the compounds; 'n' stands for number of CH₂.

CLUSTAL O(1.2.4) multiple sequence alignment

tr Q7Kwj4 Q7Kwj4_PLAF7	MDVHVNQLKNISPIDGRYKRCQEVSEYFSEYALIKYRIIVEIKWLLFLNDKEYFFPKVS	60
2QGA:B PDBID CHAIN SEQUENCE	---GSEHLKNIISPIDGRYKACGELSAFFSEHALIKHRIIVEVRWLLFLNEEELFFEKVT	57
2QGA:C PDBID CHAIN SEQUENCE	---GSEHLKNIISPIDGRYKACGELSAFFSEHALIKHRIIVEVRWLLFLNEEELFFEKVT	57
	:*****::* *:* :***:***:*****:*****:* ** **:	
tr Q7Kwj4 Q7Kwj4_PLAF7	EKLSNITSIMELINDNIDILRVKKIEEETNHDVKAVEYFIREKLESKNEEITKVIPIYVH	120
2QGA:B PDBID CHAIN SEQUENCE	DHSVEVLNQIATNITSDIARVKAIEEETNHDVKAVEYFVKEKLNKSKREDLLKIKEYVH	117
2QGA:C PDBID CHAIN SEQUENCE	DHSVEVLNQIATNITSDIARVKAIEEETNHDVKAVEYFVKEKLNKSKREDLLKIKEYVH	117
	:::.. :..* *.* ** ** * *****:***: . *.: : * : **	
tr Q7Kwj4 Q7Kwj4_PLAF7	YLCTSEDINNIAYGCLLYNCIHNIIPNIQNIIDKLKEFSFNYSVLSLKTGHQPASPT	180
2QGA:B PDBID CHAIN SEQUENCE	YLCTSEDINNVAATCLKACLNDWVIPCLEKIMLKLKDLAVEYSHVPLLSRTHGQPASST	177
2QGA:C PDBID CHAIN SEQUENCE	YLCTSEDINNVAATCLKACLNDWVIPCLEKIMLKLKDLAVEYSHVPLLSRTHGQPASST	177
	*****:.* * * :***** :*: :*****:***:***** *	
tr Q7Kwj4 Q7Kwj4_PLAF7	TFGKEMSNYYYRLYKHINKLNKIEIYVKNFNGAVGNFNAHKVCDPNIDWIDNIKYFIETYF	240
2QGA:B PDBID CHAIN SEQUENCE	TFGKEMANFYARIIHHVGVIRRVKCAKFNAGVGNFNAHKVASKDWDVNTIGLFLKKHF	237
2QGA:C PDBID CHAIN SEQUENCE	TFGKEMANFYARIIHHVGVIRRVKCAKFNAGVGNFNAHKVASKDWDVNTIGLFLKKHF	237
	*****:*:* :*:*: . : : : : : ***** . : *:*:* * :*:*:*	
tr Q7Kwj4 Q7Kwj4_PLAF7	NLHFSLYCTQIQDHDYICEISDTLARLNYTLIDLSVDMWLYISSNVLKLVKIQKEIGSST	300
2QGA:B PDBID CHAIN SEQUENCE	NLTYSIYCTQIQDHDYICELCDGLARANGTLIDLVDIWLWYISNLLKLVKKEVGSST	297
2QGA:C PDBID CHAIN SEQUENCE	NLTYSIYCTQIQDHDYICELCDGLARANGTLIDLVDIWLWYISNLLKLVKKEVGSST	297
	** :*:*****:.* * ** * *****:***:*****:***:*****	
tr Q7Kwj4 Q7Kwj4_PLAF7	MPHKVNPIDFENAEGNLHLANSFLKLFSSKLPISRLQRDLSSTVLRNLGSSFAYSLSISY	360
2QGA:B PDBID CHAIN SEQUENCE	MPHKVNPIDFENAEGNLHIANAFKLFSSKLPISRLQRDLSSTVLRNLGSSLAYCLIAY	357
2QGA:C PDBID CHAIN SEQUENCE	MPHKVNPIDFENAEGNLHIANAFKLFSSKLPISRLQRDLSSTVLRNLGSSLAYCLIAY	357
	*****:*****:.*: :***** *****:*****:***:***:***:	
tr Q7Kwj4 Q7Kwj4_PLAF7	KSLLRGLNKIDVDQNVMEQLNQNWCTLAEPQIIMKKYNIADSYELKNFTRGKSIDQK	420
2QGA:B PDBID CHAIN SEQUENCE	KSVLKGKLNKIDIDRRNLEELNQNWSTLAEPQIIMKRHNHYVDAYEELKQFTRGKVIDQK	417
2QGA:C PDBID CHAIN SEQUENCE	KSVLKGKLNKIDIDRRNLEELNQNWSTLAEPQIIMKRHNHYVDAYEELKQFTRGKVIDQK	417
	:*:***:.* :*:****** *****:***:***:***:***:***:***:***:	
tr Q7Kwj4 Q7Kwj4_PLAF7	CMYQFIQNCSHLPKNAIDELMNLTPHNYLGYASYLSKNVEHFSQEYIKKN	471
2QGA:B PDBID CHAIN SEQUENCE	IMQEFIKTKCAFLPQDWDQLLELTPATYTYGADYLAKNIVERLSGERD---	465
2QGA:C PDBID CHAIN SEQUENCE	IMQEFIKTKCAFLPQDWDQLLELTPATYTYGADYLAKNIVERLSGERD---	465
	* :**: . * : * : * : * : * : * : * : * : * : * : * : * : * : * : * : * : * : * : * : *	

Figure 2. Alignment of the amino acid sequences of *Plasmodium falciparum* ADSL and the crystal structure of 2QGA.

Abbreviation: ADSL, adenylosuccinate lyase.

** represents positions that have single, fully conserved residue; ':' indicates conservation between groups of strongly similar properties; '.' indicates conservation between groups of weakly similar properties.

Results and Discussion

Homology modelling of PfADSL and the target-template sequence alignment

A 3D structure of PfADSL was built using SWISS-MODEL with GMQE of 0.80 and QMEAN of -1.46. Also, *Plasmodium vivax* ADSL Pv003765 with AMP bound (PDB ID: 2QGA; resolution: 2.01 Å)⁵⁵ was identified to have the closest template to PfADSL with a similarity identity of 63.91% and sequence similarity of 0.50. The GMQE value of 0.80 and QMEAN score of -1.46 indicate that the modelled structure is reliable and has a good quality.^{26,28}

The multiple sequence alignment of the amino acid sequences⁵⁶ of the PfADSL (UniProtKB ID: Q7Kwj4) and *P. vivax* ADSL with AMP bound (PDB ID: 2QGA) is shown in Figure 2. A percentage identity matrix of 63.36% was obtained, which confirms the similarity identity of 63.91% obtained from the homology modelling.

Structure validation of modelled protein

The plot of the predicted local similarity to target against the residue number of the predicted 3D structure of the modelled protein was graphically represented (Figure 3A). The value of most of the residues was close to 1, indicating that the local quality estimate of the residues of the predicted model is good. The residues with values lower than 0.6 were considered to be of low quality. The modelled protein structure also lies within the range of other protein structures in PDB, which confirms its reliability (Figure 3B).

Both the Ramachandran plot (Figure 4A) and the Ramachandran plot statistics (Figure 4B) were obtained from PDBsum web server. The Ramachandran plot statistics implied that the modelled 3D structure of PfADSL has 91.8% of its residues in the most favoured regions, 7.4% of its residues in additional allowed regions, 0.8% of its residues in the generously allowed regions and 0.0% of its residues in disallowed regions of the Ramachandran plot. This also validates that the

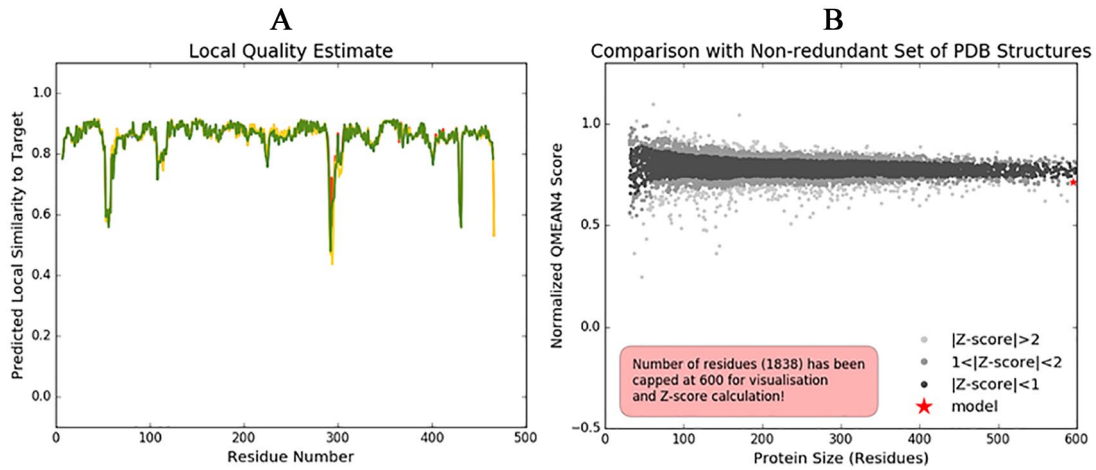


Figure 3. Structure validation of modelled *PfADSL*: (A) Local quality estimate of the residues of the predicted *PfADSL* model; (B) comparison of the predicted *PfADSL* structure with nonredundant set of PDB structures. Abbreviation: *PfADSL*, *Plasmodium falciparum* adenylsuccinate lyase, PDB, Protein Data Bank.

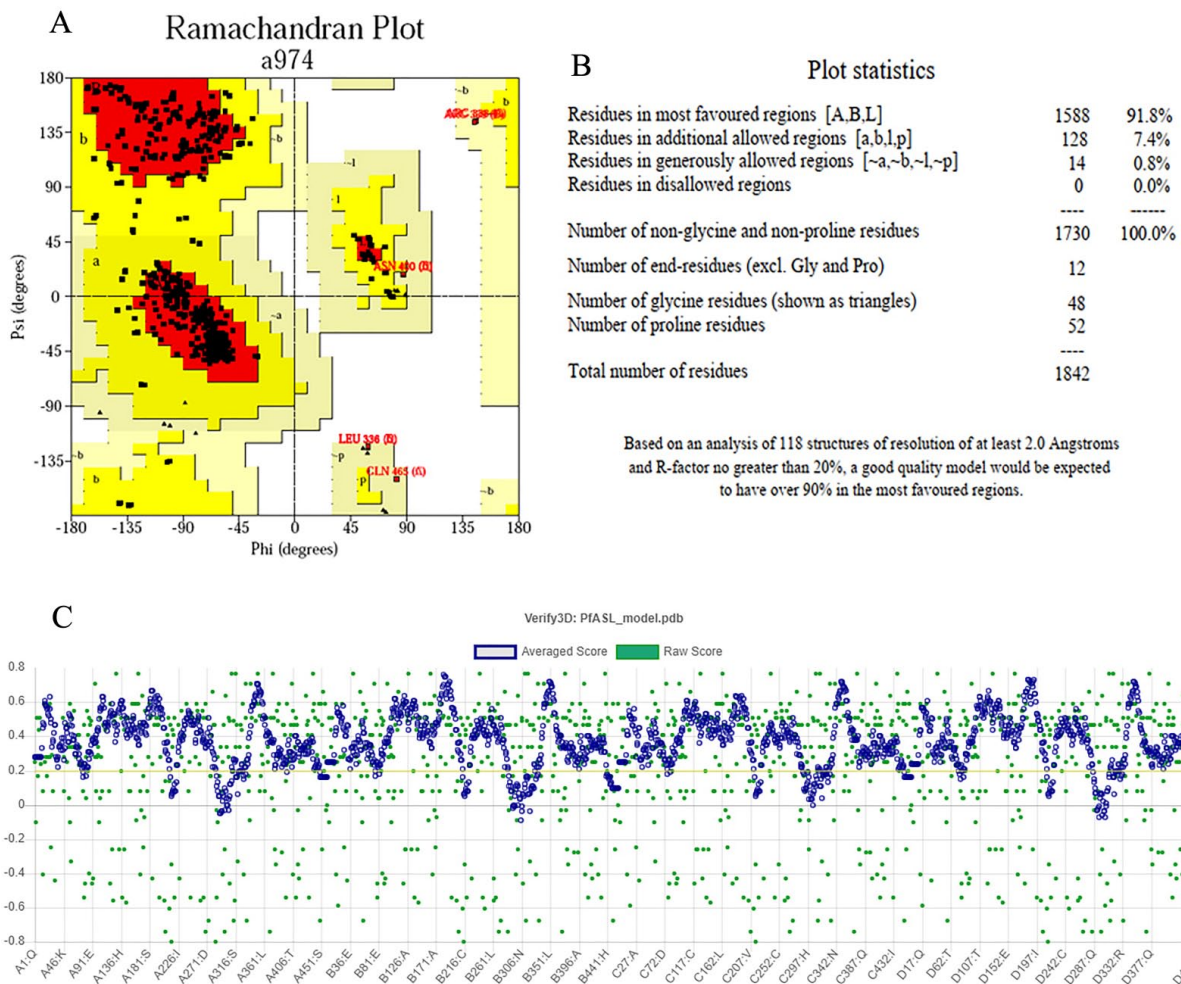


Figure 4. Structure validation using (A) Ramachandran plot; (B) Ramachandran plot statistics of the homology modelled *PfADSL*; and (C) Verify3D. Abbreviation: *PfADSL*, *Plasmodium falciparum* adenylsuccinate lyase.

modelled 3D structure is a good quality model. Also, the Verify3D plot of the modelled protein (Figure 4C) was obtained for the structure validation and it showed as PASS.

The 3D environment profile shows that 85.64% of the residues have averaged 3D-1D score ≥ 0.2 , which suggests the validity of the modelled protein.

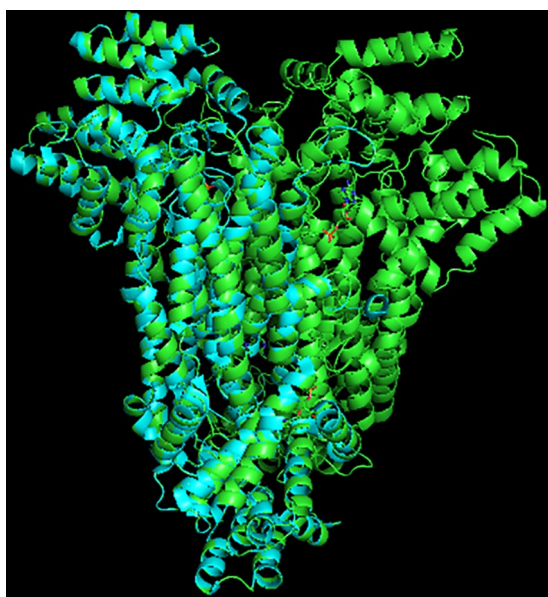


Figure 5. Alignment of the PfADSL model and the 2GQA template structure of *Plasmodium vivax* ADSL.

Abbreviation: PfADSL, *Plasmodium falciparum* adenylosuccinate lyase.

Alignment of the PfADSL model and template (2GQA) structure

A RMSD value of 0.105 Å was obtained from the alignment computed using PyMOL molecular viewer, indicating that the structures were closely related (Figure 5). The template structure is represented by the blue helices, whereas the protein model is represented by the green helices. The alignment showed that the chain B and chain C of the dimer template structure (2QGA) corresponded to the chain C and chain D of the tetramer structure of the protein model. Meanwhile, it was observed from the molecular viewer that the binding of the AMP to the amino acid residues of 2QGA at His 168B, Asn 85C, Asp 87C, Gln 245C, Ser 338C, Arg 333C and Arg 342D also corresponded with the binding of the AMP with the amino acid residues of the modelled template at His 173C, Asn 90D, Asp 92D, Gln 250D, Ser 343D, Arg 338D and Arg 347D.

In silico results of risks and drug-likeness of ligands

a. OSIRIS property explorer result. With the exception of compound **4c**, all the predicted toxicity risk factors for the 8 designed substituted benzo[*d*]imidazol-1-yl)methyl)benzimidamides were low (Table 1). Also, the 8 compounds had molecular weights less than 500, which implied that they are likely to be absorbed and are able to reach the place of action when administered as drugs.⁵⁷ All compounds including the standard drug (chloroquine) had LogP values not higher than 5, suggesting good absorption and permeation across cell membranes.⁵⁷ Among the compounds, 4-((2-benzyl-1H-benzo[*d*]imidazol-1-yl)methyl)benzimidamide **4f** had the highest value of drug score (0.83), which is higher than

Table 1. Physicochemical properties and toxicity risks of compounds **4a-h** in comparison with chloroquine as predicted using OSIRIS Property Explorer.

COMPOUNDS	PHYSICO-CHEMICAL PROPERTIES					TOXICITY RISKS				
	MOLECULAR WEIGHT	CLOGP	SOLUBILITY PREDICTION	DRUG LIKENESS	DRUG SCORE	MUTAGENIC	TUMORIGENIC	IRRITANT	REPRODUCTIVE EFFECTIVE	
4a	326	3.08	-3.69	4.09	0.78	Low	Low	Low	Low	
4b	360	3.69	-4.43	3.68	0.67	Low	Low	Low	Low	
4c	356	1.73	-3.85	-1.17	0.30	High	Low	Low	Low	
4d	342	2.74	-3.40	3.14	0.80	Low	Low	Low	Low	
4e	341	2.40	-3.77	0.93	0.69	Low	Low	Low	Low	
4f	340	3.14	-2.54	3.63	0.83	Low	Low	Low	Low	
4g	352	3.53	-2.97	2.11	0.75	Low	Low	Low	Low	
4h	341	2.40	-3.77	1.36	0.72	Low	Low	Low	Low	
Chloroquine	319	4.01	-4.06	7.39	0.25	High	Low	High	Low	

Table 2. ADME prediction of compounds **4a-h** in comparison with chloroquine, predicted by SwissADME.

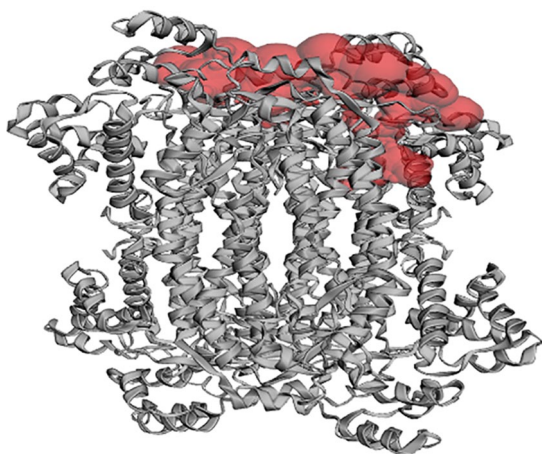
COMPOUNDS	FORMULA	NHD	NHA	NRB	TPSA (Å ²)	LOGP (ILOGP)	LOGS (ESOL)	SYNTHETIC ACCESSIBILITY
4a	C ₂₁ H ₁₈ N ₄	2	2	4	67.69	2.27	-4.53	2.44
4b	C ₂₁ H ₁₇ ClN ₄	2	2	4	67.69	2.11	-5.11	2.54
4c	C ₂₁ H ₂₀ N ₆	4	2	4	119.73	1.38	-3.81	2.74
4d	C ₂₁ H ₁₈ N ₄ O	3	3	4	87.92	2.11	-4.38	2.52
4e	C ₂₁ H ₁₉ N ₅	3	2	4	93.71	2.00	-4.17	2.62
4f	C ₂₂ H ₂₀ N ₄	2	2	5	67.69	2.11	-4.17	2.62
4g	C ₂₃ H ₂₀ N ₄	2	2	5	67.69	2.34	-4.98	2.89
4h	C ₂₁ H ₁₉ N ₅	3	2	4	93.71	1.81	-4.17	2.60
Chloroquine	C ₁₈ H ₂₆ ClN ₃	1	2	8	28.16	3.95	-4.55	2.76

Abbreviations: ADME, absorption, distribution, metabolism, excretion; NHA, no. of hydrogen bond acceptors; NHD, no. of hydrogen bond donors; NRB, no. of rotatable bonds; TPSA, total polar surface area.

Table 3. Energy-based interactions and hydrogen bonds for benzimidazole derivatives **4a-h**, AICAR and AMP docked into modelled *PfADSL*.

COMPOUNDS	BINDING ENERGIES (KCAL/MOL)	HYDROGEN BONDS AND THE BOND LENGTHS
4a	-7.52	Ser 298A (3.01 Å), Ser 299A (3.19 Å)
4b	-7.85	Ser 298A (3.17 Å), Ser 299A (2.98 Å)
4c	-6.85	Asn 90D (2.90 Å), Thr 124D (2.90 Å), Thr 300A (2.67 Å)
4d	-7.03	Ser 298A (2.87 Å), Ser 299A (3.10 Å), Thr 124D (2.79 Å)
4e	-7.48	Gln 250D (3.05 Å), Ile 296A (2.71 Å)
4f	-8.09	Glu 295A (2.46 Å), Asn 306A (2.70 Å)
4g	-8.75	Ser 299A (3.02 Å), Thr 124D (2.97 Å)
4h	-7.20	Ser 298A (3.17 Å), Ser 299A (3.25 Å), Asp 92D (2.77 Å)
AICAR	-5.49	Ser 298A (2.92 Å), Ser 299A (2.81 Å), His 91D (3.04 Å), Thr 172C (2.76 Å), Lys 304A (2.96 Å), His 173C (2.90 Å)
AMP	-5.10	Tyr 18A (2.56 Å), Asn 312A (3.04 Å), Arg 17A (2.94 Å), Asn 90D (2.72 Å), Gln 250D (2.72 Å), Arg 338D (3.01 Å), Ser 343D (2.95 Å), Arg 347 (2.76 Å)

Abbreviations: AICAR, 5-aminoimidazole-4-carboxamide ribonucleotide; AMP, adenosine monophosphate.

**Figure 6.** The surface of the binding pocket of the modelled protein as computed using CASTp 3.0.

that of chloroquine (0.25). This high value could be as a result of the aliphatic carboxylic acid (phenyl acetic acid) on position 2 of the benzimidazole in **4f**. In general, the drug score values of compounds **4a-h** (0.3-0.83) were bigger than that of chloroquine. In addition, it was predicted that all the designed compounds possessed low mutagenic, tumorigenic, irritant and reproductive effective toxicity risks except **4c**, which was predicted to have a high mutagenic toxicity risk. However, the removal of the amino group on position 5 of the benzoic acid as seen in **4h** reduced the risk of the mutagenic toxicity of **4c**.

b. SwissADME prediction. The numbers of hydrogen bond acceptors (NHA) and hydrogen bond donors (NHD) in compounds **4a-h** (Table 2) are in accordance with the rule of five by Lipinski et al.³⁷ The LogS prediction of -5.11 to -3.81

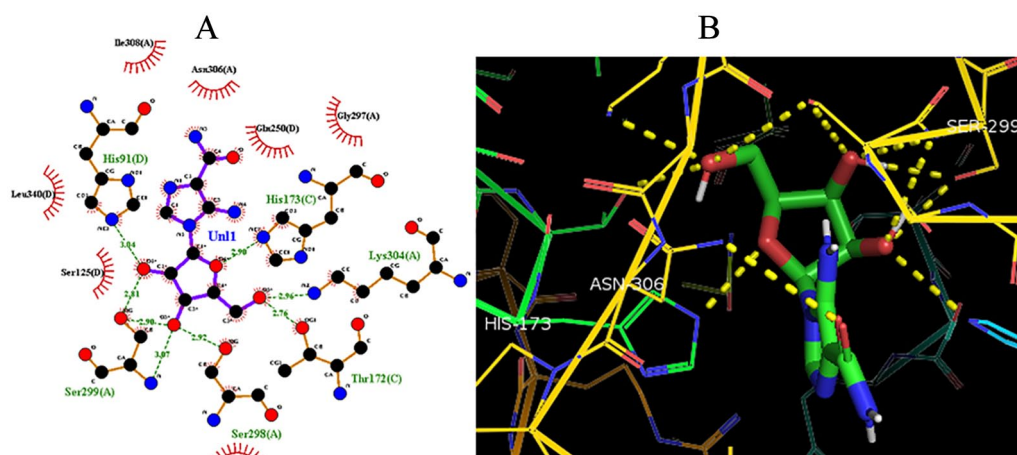


Figure 7. Molecular docking interactions between AICAR and the binding sites of *PfADSL*: (A) 2D model of the interactions between AICAR and *PfADSL*; (B) 3D model of the interactions between AICAR and the binding sites of *PfADSL*.
Abbreviation: AICAR, 5-aminoimidazole-4-carboxamide ribonucleotide; *PfADSL*, *Plasmodium falciparum* adenylosuccinate lyase.

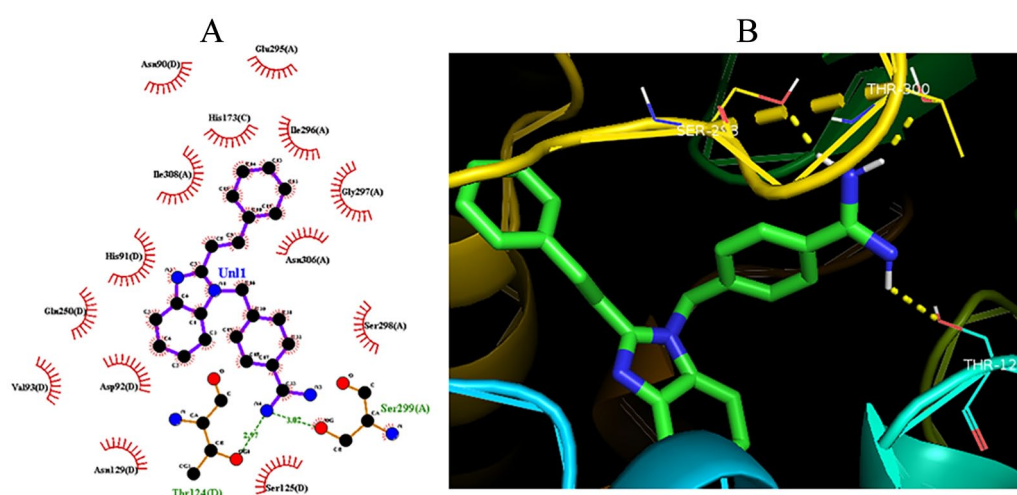


Figure 8. Molecular docking interactions between **4g** and the binding sites of *PfADSL*: (A) 2D model of the interactions; (B) 3D model of the interactions.
Abbreviation: *PfADSL*, *Plasmodium falciparum* adenylosuccinate lyase.

indicated that all the compounds were moderately soluble. Also, the highest value (2.89) of synthetic accessibility was recorded for compound **4g**, suggesting that it will be the most difficult to synthesise from the compound library. This could be due to the presence of a double bond in position 2 of the benzimidazole. Generally, the synthetic accessibility of all the compounds (2.44–2.89) was within the range of easy synthetic accessibility. It is also interesting to note that none of the compounds violated the Lipinski rule of five, Ghose filter, Veber rule, Egan rule and Muegge rule. This shows that all the ligands can be considered as good lead compounds in drug design.

Active site identification

From the active site prediction, a pocket was identified with an area (SA) of 2919.055 and a volume (SA) of 2797.556 (Figure 6). A total of 166 amino acid residues were predicted to be the

active sites for the modelled protein. However, the following were chosen as the more favourable sites for the docking analyses due to the similarities observed from the alignment of the modelled structure to the template structure: Arg 17A, Tyr 18A, Asn 312A, His 173C, Asn 90D, Asp 92D, Gln 250D, Arg 338D, Ser 343D, Arg 347D.

Molecular docking results

The obtained binding energies and hydrogen bonds of compounds **4a–h** from the molecular docking simulations are detailed in Table 3, whereas the docked conformation of AICAR and (*E*)-4-((2-styryl-1H-benzo[d]imidazol-1-yl)methyl)benzimidamide (**4g**) in the active sites of *PfADSL* is presented in Figures 7 and 8, respectively. Structure–activity relationship studies based on the observed dock score values of the compounds suggest that the presence of amidine group, RC(=NH)-NH₂, on the compounds could be responsible for

the low binding energies and strong binding affinity (Table 3). Also, the presence of amino group on position 2 of the substituted phenyl in **4e** (−7.48 kcal/mol) increased the binding affinity of the compound as against it being on position 3 as observed in **4h** (−7.20 kcal/mol). The di-substitution of amino groups on positions 3 and 5 of the substituted phenyl in **4e** did not have a positive impact on the binding energy but rather reduced its binding affinity (−6.85 kcal/mol) as against the mono-substitutions on position 2 of **4e** and position 3 on **4h**.

Furthermore, all the designed compounds exhibited dock score values between −6.85 and −8.75 kcal/mol, having lower binding energies than that of the complexed ligand (AMP) that had a binding energy of −5.10 kcal/mol. Also, the binding energies of the compounds were lower than AICAR (−5.49 kcal/mol), which has been reported to be a potential inhibitor of *Pf*ADSL.⁷ The lowest autodock score and the best interactions were used to ascertain the compound with the best conformation.² The best dock score among the designed benzimidazole derivatives was −8.75 kcal/mol for compound **4g**. The hydrogen bond formed between compound **4g** and the amino acid residues (Ser 299A, Thr 124D) of *Pf*ADSL also validates the functional and structural stability of the ligand-protein complex.² Thus, the binding model reported in this study suggests that these substituted benzo[*d*]imidazol-1-yl)methyl)benzimidamides behave as *Pf*ADSL inhibitors and show some key structural points to be considered in future optimization.

Conclusion

*Pf*ADSL is a potential drug target that can be considered in the design of antimalarial compounds to combat the malaria menace. This study gives an insight into the design and prediction of potential interaction modes and binding affinities of 8 substituted benzo[*d*]imidazol-1-yl)methyl)benzimidamide compounds with homology modelled *Pf*ADSL. (*E*)-4-((2-styryl-1H-benzo[*d*]imidazol-1-yl)methyl)benzimidamide, **4g**, had the highest dock score value among the designed ligands. All the designed compounds possessed good in silico ADMET properties, demonstrating their safety for further synthesis and development into active commercially available antimalarial drugs. Also, experimental characterization is needed for further validation of the protein target.

Acknowledgements



The authors acknowledge Covenant University for the infrastructural support of this work and also thank Jide Ayodele of Covenant University Bioinformatics Research (CUBRe) for assisting with logistics.

Author Contributions

BB and EA determined the choice of the protein target. EA, OOA, and GOO put up the general concepts and design of the study. GOO carried out the implementation of these concepts. GOO, OOA, YUA and EA carried out the analysis of the

work. GOO wrote the paper. GOO, OOA, YUA and EA revised the manuscript.

ORCID iDs

Olayinka O Ajani  <https://orcid.org/0000-0002-3422-3478>
Ezekiel Adebisi  <https://orcid.org/0000-0002-1390-2359>

REFERENCES

- Durojaye OA, Ilo CC, Okeowhor D, et al. The malaria concept in pregnancy and the mechanism of evading the immune system by the malaria parasite. *South Asian J Parasitol.* 2019;2:1–7.
- Singh IV, Mishra S. Molecular docking studies of benzamide derivatives for PfDHODH inhibitor as potent antimalarial agent. *Am J Biochem Molec Biol.* 2019;9:1–6.
- Reynolds JJ. *Structure-Based Drug Discovery Against a Novel Antimalarial Drug Target, S-Adenosylmethionine Decarboxylase/Ornithine Decarboxylase* [Doctoral dissertation]. Pretoria, South Africa: University of Pretoria; 2013.
- Pasupureddy R, Seshadri S, Pande V, Dixit R, Pandey KC. Current scenario and future strategies to fight artemisinin resistance. *Parasitol Res.* 2019;118:29–42.
- Jurecka A, Zikanova M, Kmoch S, Tylki-Szymańska A. Adenylosuccinate lyase deficiency. *J Inherit Metabol Dis.* 2015;38:231–242.
- Bulusu V, Srinivasan B, Bopanna MP, Balaran H. Elucidation of the substrate specificity, kinetic and catalytic mechanism of adenylosuccinate lyase from *Plasmodium falciparum*. *Biochim Biophys Acta.* 2009;1794:642–654.
- Cassera MB, Zhang Y, Hazleton KZ, Schramm VL. Purine and pyrimidine pathways as targets in *Plasmodium falciparum*. *Curr Top Med Chem.* 2011;11:2103–2115.
- Sharma K, Shrivastava A, Mehra RN, et al. Synthesis of novel benzimidazole acrylonitriles for inhibition of *Plasmodium falciparum* growth by dual target inhibition. *Arch Pharm (Weinheim).* 2018;351:1700251.
- Tonelli M, Gabriele E, Piazza F, et al. Benzimidazole derivatives endowed with potent antileishmanial activity. *J Enzyme Inhib Med Chem.* 2018;33:210–226.
- Cheretaev IV, Korenyuk II, Nozdrachev AD. Neurotropic, psychoactive, and analgesic properties of benzimidazole and its derivatives: physiological mechanisms. *Neurosci Behav Physiol.* 2018;48:848–853.
- Cheong JE, Zaffagni M, Chung I, et al. Synthesis and anticancer activity of novel water soluble benzimidazole carbamates. *Eur J Med Chem.* 2018;144:372–385.
- Rashid N, Kiran A, Ashraf Z, et al. Synthesis, characterization, antitumor, antibacterial and urease inhibitory activity of a small series of N-tosyl benzimidazoles. *J Chem Soc Pakistan.* 2018;40:366–375.
- Manju PT, Smith AA, Padmaja V, et al. In silico design, synthesis and in vitro anti-tubercular and anti-microbial screening of novel benzimidazole derivatives. *Int J Pharmaceut Sci Res.* 2018;9:3705–3711.
- Kumar PL, Bharathi T, Aravind K, et al. Synthesis and anti-inflammatory activity of N-(2-(1H-indol-2-yl)-1H-benzimidazol-1-yl)benzamide. *World J Pharm Pharmaceut Sci.* 2018;7:776–783.
- Patil VM, Gupta SP. Structural flexibility in HCV NS5B polymerase and molecular modelling of anti-HCV drugs. *Curr Chem Biol.* 2018;12:65–87.
- Majewsky M, Castel D, Le Dret L, et al. Systematic identification of suspected anthelmintic benzimidazole metabolites using LC–MS/MS. *J Pharm Biomed Anal.* 2018;151:151–158.
- Bistrovic A, Krstulovic L, Stolic I, et al. Synthesis, anti-bacterial and anti-protazoal activities of amidinobenzimidazole derivatives and their interactions with DNA and RNA. *J Enzyme Inhib Med Chem.* 2018;33:1323–1334.
- Pomel S, Dubar F, Forge D, Loiseau PM, Biot C. New heterocyclic compounds: synthesis and antitrypanosomal properties. *Bioorg Med Chem.* 2015;23:5168–5174.
- Singh P, Kumari K, Awasthi SK, Chandra R. Virtual screening and docking studies of synthesised chalcones: potent anti-malarial drug. *Int J Drug Dev Res.* 2016;8:49–56.
- Barcellos MP, Santos CB, Federico LB, Almeida PF, da Silva CHTP, Taft CA. Pharmacophore and structure-based drug design, molecular dynamics and admet/tox studies to design novel potential pad4 inhibitors. *J Biomol Struct Dyn.* 2019;37:966–981.
- Muhammed MT, Aki-Yalcin E. Homology modeling in drug discovery: overview, current applications, and future perspectives. *Chem Biol Drug Des.* 2019;93:12–20.
- Ugwu DI, Okoro UC, Ukoha PO, Okafor S, Ibezim A, Kumar NM. Synthesis, characterisation, molecular docking and in vitro antimalarial properties of new carboxamides bearing sulphonamide. *Eur J Med Chem.* 2017;135:349–369.

23. Burley SK, Berman HM, Bhikadiya C, et al. RCSB Protein Data Bank: biological macromolecular structures enabling research and education in fundamental biology, biomedicine, biotechnology and energy. *Nucleic Acids Res.* 2018;47:D464–D474.
24. UniProt Consortium. UniProt: a worldwide hub of protein knowledge. *Nucleic Acids Res.* 2018;47:D506–D515.
25. Waterhouse A, Bertoni M, Bienert S, et al. SWISS-MODEL: homology modelling of protein structures and complexes. *Nucleic Acids Res.* 2018;46:W296–W303.
26. Cardoso JM, Fonseca L, Egas C, Abrantes I. Cysteine proteases secreted by the pinewood nematode, *Bursaphelenchus xylophilus*: in silico analysis. *Comput Biol Chem.* 2018;77:291–296.
27. Benkert P, Kunzli M, Schwede T. QMEAN server for protein model quality estimation. *Nucleic Acids Res.* 2009;37:W510–W514.
28. Patel B, Singh V, Patel D. Structural Bioinformatics. In: Shaik, NA, Hakeem, KR, Banganapalli, B, et al., eds. *Essentials of Bioinformatics*, vol. I. Cham, Switzerland: Springer; 2019:169–199.
29. Sainy J, Sharma R. Synthesis, antimalarial evaluation and molecular docking studies of some thiolactone derivatives. *J Molec Struct.* 2017;1134:350–359.
30. Laskowski RA. PDBsum new things. *Nucleic Acids Res.* 2008;37:D355–D359.
31. Laskowski RA, MacArthur MW, Moss DS, Thornton JM. PROCHECK: a program to check the stereochemical quality of protein structures. *J Appl Crystal.* 1993;26:283–291.
32. Eisenberg D, Lüthy R, Bowie JU. [20] VERIFY3D: assessment of protein models with three-dimensional profiles. *Methods Enzymol* 1997;277:396–404.
33. De Lano WL. Pymol: an open-source molecular graphics tool. *CCP4 Newsletter Protein Crystal.* 2000;40:82–92.
34. Leite TB, Gomes D, Miteva MA, Chomilier J, Villoutreix BO, Tuffery P. FROG: a FRee Online druG 3D conformation generator. *Nucleic Acids Res.* 2007;35:W568–W572.
35. O'Boyle NM, Banck M, James CA, Morley C, Vandermeersch T, Hutchison GR. Open Babel: an open chemical toolbox. *J Cheminform.* 2011;3:33.
36. Egbert M, Whitty A, Keseru GM, Vajda S. Why some targets benefit from beyond rule of five drugs [published online ahead of print June 12, 2019]. *J Med Chem.* doi:10.1021/acs.jmedchem.8b01732.
37. Lipinski CA, Lombardo F, Dominy BW, Feeney PJ. Experimental and computational approaches to estimate solubility and permeability in drug discovery and development settings. *Adv Drug Delivery Rev.* 2012;64:4–17.
38. Behrouz S, Rad MN, Shahraki BT, Fathalipour M, Behrouz M, Mirkhani H. Design, synthesis, and in silico studies of novel eugenylxyloxy propanol azole derivatives having potent antinociceptive activity and evaluation of their β -adrenoceptor blocking property. *Molec Diversity.* 2019;23:147–164.
39. Torres E, Moreno E, Ancizu S, et al. New 1,4-di-N-oxide-quinoxaline-2-yl-methylene isonicotinic acid hydrazide derivatives as anti-mycobacterium tuberculosis agents. *Bioorg Med Chem Lett.* 2011;21:3699–3703.
40. Daina A, Michielin O, Zoete V. SwissADME: a free web tool to evaluate pharmacokinetics, drug-likeness and medicinal chemistry friendliness of small molecules. *Sci Rep.* 2017;7:42717.
41. Lohidakshan K, Rajan M, Ganesh A, Paul M, Jerin J. Pass and Swiss ADME collaborated in silico docking approach to the synthesis of certain pyrazoline spacer compounds for dihydrofolate reductase inhibition and antimalarial activity. *Bangladesh J Pharmacol.* 2018;13:23–29.
42. Mahato S, Singh A, Rangan L, Jana CK. Synthesis, in silico studies and in vitro evaluation for antioxidant and antibacterial properties of diarylmethylamines: a novel class of structurally simple and highly potent pharmacophore. *Eur J Pharm Sci.* 2016;88:202–209.
43. Muegge I, Heald SL, Brittelli D. Simple selection criteria for drug-like chemical matter. *J Med Chem.* 2001;44:1841–1846.
44. Ghose AK, Viswanadhan VN, Wendoloski JJ. A knowledge-based approach in designing combinatorial or medicinal chemistry libraries for drug discovery. 1. A qualitative and quantitative characterization of known drug databases. *J Comb Chem.* 1999;1:55–68.
45. Egan WJ, Merz KM Jr, Baldwin JJ. Prediction of drug absorption using multivariate statistics. *J Med Chem.* 2000;43:3867–3877.
46. Veber DF, Johnson SR, Cheng HY, Smith BR, Ward KW, Kopple KD. Molecular properties that influence the oral bioavailability of drug candidates. *J Med Chem.* 2002;45:2615–2623.
47. Pettersen EF, Goddard TD, Huang CC, et al. UCSF Chimera – a visualization system for exploratory research and analysis. *J Comput Chem.* 2004;25:1605–1612.
48. Singh IV, Mishra S. Molecular docking analysis of Pyrimethamine derivatives with *Plasmodium falciparum* dihydrofolate reductase. *Bioinformation.* 2018;14:232–235.
49. Tian W, Chen C, Lei X, Zhao J, Liang J. CASTp 3.0: computed atlas of surface topography of proteins. *Nucleic Acids Res.* 2018;46:W363–W367.
50. Dundas J, Ouyang Z, Tseng J, Binkowski A, Turpaz Y, Liang J. CASTp: computed atlas of surface topography of proteins with structural and topographical mapping of functionally annotated residues. *Nucleic Acids Res.* 2006;34:W116–W118.
51. Toth EA, Yeates TO. The structure of adenylosuccinate lyase, an enzyme with dual activity in the de novo purine biosynthetic pathway. *Structure.* 2000;8:163–174.
52. Yang J, Wang Y, Woolridge EM, et al. Crystal structure of 3-carboxy-cis, cis-muconate lactonizing enzyme from *Pseudomonas putida*, a fumarase class II type cycloisomerase: enzyme evolution in parallel pathways. *Biochemistry.* 2004;43:10424–10434.
53. Morris GM, Huey R, Lindstrom W, et al. AutoDock4 and AutoDockTools4: automated docking with selective receptor flexibility. *J Comput Chem.* 2009;30:2785–2791.
54. Laskowski RA, Swindells MB. LigPlot+: multiple ligand–protein interaction diagrams for drug discovery. *J Chem Inf Model.* 2011;51:2778–2786.
55. Lunin VV, Wernimont AK, Lew J, et al. *Plasmodium vivax* adenylosuccinate lyase Pv003765 with AMP bound, <https://www.thesgc.org/structures/2qga>
56. Goujon M, McWilliam H, Li W, et al. A new bioinformatics analysis tools framework at EMBL–EBI. *Nucleic Acids Res.* 2010;38:W695–W699.
57. Wu CY, Benet LZ. Predicting drug disposition via application of BCS: transport/absorption/elimination interplay and development of a biopharmaceutics drug disposition classification system. *Pharm Res.* 2005;22:11–23.